Modeling of a coupled fluid-structure system excited by piezoelectric actuators

Flávio Luiz Cardoso-Ribeiro, Valérie Pommier-Budinger, Jean-Sebastien Schotte, Denis Arzelier

Modeling of a coupled fluid-structure system excited by piezoelectric actuators

Flavio Luiz Cardoso-Ribeiro[1], Valerie Pommier-Budinger[2], Jean-Sebastien Schotte[3] and Denis Arzelier[4]

***Abstract*— Structural vibrations can have severe consequences on airplane design like fatigue, aeroelastic instability and reduced manoeuvrability. Fuel sloshing inside wing tanks can increase these problems. This work is intended to model a system that consists of a cantilever aluminum plate with a fluid tank near the free tip. Piezoelectric patches are used to excite the system. Three different methodologies were used to obtain a state-space model of the system: analytical (exact) solutions of simplified problems, numerical approximated methods and system identification techniques. Results show good agreement between theory and experiments.**

I. INTRODUCTION

One of the main characteristics of each new generation of airplanes design is the constant goal of reducing total weight. This goal inevitably leads to an increase in the structural flexibility. Sloshing of fuel in large jet airplanes can cause vibration which interacts with the flexible wing, and can lead to problems related to the maneuverability of the aircraft, fatigue and instabilities. This work focuses on the use of piezoelectric patches for rejection of vibrations on this type of system.

To study this problem, we use an experimental device, which consists of a cantilevered plate with a tank partially filled with fluid near the tip. The experimental device can be seen as a simplified experimental model of a very flexible wing with tip fuel tank. Piezoelectric patches are used as actuators. Various types of measurement output can be considered (as the measurement given by an accelerometer or a piezoelectric transducer).

This work is a continuation and extension of the thesis of Bogdan Robu (Refs. [16], [17]). Robu studied a cantilevered flexible plate with a fuel tank attached to the tank tip. Piezoelectric patches were used both as actuators and sensors. The final goal was to use feedback control to attenuate the structural vibration and fluid sloshing. His first challenge was to define how to mathematically model the system. For structural dynamics, a plate model was used. He used "assumed modes" method to find a finite-dimension representation. The sloshing dynamics was then addressed by using a rectangular tank approximation. A finite-dimension representation was obtained using an analogy with a mass-pendulum system. Both dynamics were then represented as a set of coupled ordinary differential equations. Finally, he used HIFOO Toolbox (Refs. [5] and [6]) to find a low-order controller, capable of attenuating vibrations of the first modes.

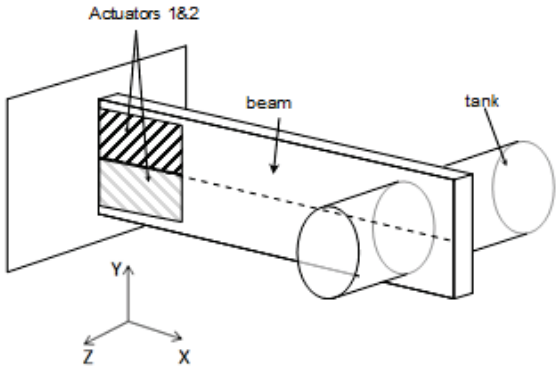

Fig. 1. Experimental set up.

Previous work lacked of accurate modeling and experimental validation of the full experimental device. In Ref. [16], differences between experimental and theoretical results were solved by model matching (natural frequencies were obtained directly from experiments, instead of theoretical model). It is clear that more effort needs to be addressed concerning the modeling of the coupling between structural dynamics and fuel sloshing and validation with experimental results.

In this work, we tried to use the simplest mathematical formulation as possible to describe the experiment. A simple beam formulation was used to describe the plate. Piezoelectric effect was added as generalized force/moment, as described in Ref. [13].

As done in previous work, we used a simple inviscid sloshing model in a rectangular tank (Refs. [1], [2], [7], [9], [11], [15]). This model is convenient since it is one of the only approaches that leads to an analytical model (more complicated sloshing models can only be solved by numerical methods). Despite the simplifications, this method allows a good approximation concerning the sloshing modal frequencies.

Our contribution concerns the modeling of the full experimental device by coupling the structural dynamics with the sloshing equations, the validation of the theoretical frequency response by experimental measurements and the analysis of

[1]F.C. Cardoso-Ribeiro is a Ph.D. candidate at Université de Toulouse/ ISAE - 10, Avenue Edouard Belin, 31055 Toulouse, with a scholarship from CNPq - Brazil. flaviocr@ita.br

[2] V. Pommier-Budinger is with Université de Toulouse/ ISAE - 10, Avenue Edouard Belin, 31055 Toulouse France valerie.budinger@isae.fr

[3] J.S. Schotte is with ONERA, Chatillon, France jean-sebastien.schotte@onera.fr

[4] D. Arzelier is with Laboratoire d'Analyse et d'Architecture des Systmes /LAAS-CNRS, 7, Avenue du Colonel Roche, 31400 Toulouse - France arzelier@laas.fr

the limit of the model.

Sections II and III show how to obtain a state-space representation for the beam and for sloshing dynamics, respectively. Then, both representations are coupled in Section IV. Finally, Section V presents the results and comparisons between the analytical, numerical and experimental methods.

II. STRUCTURAL DYNAMICS

In this section, we show the mathematical model of a beam in bending and torsion. Voltage applied to piezoelectric patches and point-forces are used as inputs of the system.

A. Bending equations

The following equation, derived from Euler-Bernoulli equation, can represent the dynamic behaviour of a uniform beam in bending (Ref. [14]):

$$EI\frac{\partial^4 w}{\partial x^4} = -\mu\frac{\partial^2 w}{\partial t^2} + q(x,t), \quad 0 \leq x \leq L. \tag{1}$$

where x is the position along the beam, L is the beam length, $w = w(x,t)$ is the beam deflection, E is the material Young's modulus, I is the second moment of area, $q(x,t)$ is the force applied per unit lenght, μ is the mass per unit lenght.

In the case of a beam clamped in a wall at $x = 0$ and free at $x = L$, we have the following boundary conditions: At the clamped end:$w(0,t) = 0$, $\frac{\partial w}{\partial x}(0,t) = 0$; at the free end: $EI\frac{\partial^2 w}{\partial x2}(L,t) = 0$,$\frac{\partial}{\partial x}\left[EI\frac{\partial^2 w}{\partial x2}(L,t)\right] = 0$.

The dynamic equations can be solved using modal decomposition as a set of independent ordinary differential equations (for the case of zero initial conditions). The solution $w(x,t)$ is given as an infinite sum and approximating by truncating on the "n-th" term:

$$w(x,t) = \sum_{i=1}^{\infty} W_i(x)T_i^w(t) \approx \sum_{i=1}^{n} W_i(x)T_i^w(t), \tag{2}$$

Where $T_i^w(t)$ is $i-th$ bending mode displacement. It is given by a system of second order ordinary differential equations:

$$\ddot{T_i^w}(t) + \omega_i^2 T_i^w(t) = F_i, \tag{3}$$

where $\ddot{T_i^w}(t) = \frac{\partial^2 T_i^w(t)}{\partial t^2}$, ω_i is the i-th bending mode's natural frequency, F_i is the generalized external force applied to mode i. The natural frequency is given by: $\omega_i = \beta_i^2\sqrt{\frac{EI}{\mu}}$, where β is the solution of the following equation: $\cos(\beta L)\,\cosh(\beta L) + 1 = 0$.

The generalized forces can be calculated from the modal shapes and external forces. In the case of a point force $q(t)$ perpendicular to the beam, at position x_f, F_i is given by:

$$F_i(t) = W_i(x_f)q(t) \tag{4}$$

It's possible to re-write Eq. 3 as:

$$\dot{X} = \mathbf{A}X + \mathbf{B}u \tag{5}$$

where $X = \begin{bmatrix} \dot{T}_i^w & T_i^w \end{bmatrix}$, $u = q(t)$.

Choosing as output the tip deflection:

$$Y = w(L,t) = \sum_{i=1}^{\infty} W_i(L)T_i^w(t) \approx \sum_{i=1}^{n} W_i(L)T_i^w(t). \tag{6}$$

It is possible to write it in the matrix form:

$$Y = \mathbf{C}X. \tag{7}$$

From these equations, we see that matrix **A** can be obtained from the modes natural frequencies, and matrices **B** and **C** are directly obtained from the modal shapes.

B. Torsion - shaft dynamics

The torsion dynamics of a uniform beam can be approximated by (See Refs. [4], [10]):

$$GJ\frac{\partial^2\theta(x,t)}{\partial x^2} + m(x,t) = I\frac{\partial^2\theta(x,t)}{\partial t^2}, \quad 0 \leq x \leq L. \tag{8}$$

where $\theta(x,t)$ is the local torsion angle, x is the position along the beam, t is time, $m(x,t)$ is the local external torsion moment, G is the material shear constant, J is the section torsion constant and I is the section polar moment of inertia per unit lenght.

Here we are dealing with a clamped-free beam. The boundary conditions are given by: condition on the clamped tip (no displacement): $\theta(x,t) = 0, \quad at \quad x = 0$; Free condition: $G(x)J(x)\frac{\partial\theta(x,t)}{\partial x} = 0, \quad at \quad x = L$.

As in the bending case, the dynamic equations can be solved using modal decomposition:

$$\ddot{T_i^\theta}(t) + \omega_i^2 T_i^\theta(t) = M_i, \tag{9}$$

where $T_i^\theta(t)$ is i-th torsion mode displacement, ω_i is the i-th torsion mode natural frequency, M_i is the generalized external force applied to mode i.

The angular displacement at any position x can then be calculated from:

$$\theta(x,t) = \sum_{i=0}^{\infty} \Theta_i(x)T_i^\theta(t) \approx \sum_{i=0}^{n} \Theta_i(x)T_i^\theta(t). \tag{10}$$

Where $\Theta_i(x)$ is the eigenfunction and w_i the modal natural frequency, given by: $\omega_i = i\frac{\pi}{2}\sqrt{\frac{GJ}{IL^2}}, \quad i = 1,3,....$

C. Piezoelectric patches effect

Piezoelectric patches can be modelled as a generalized force and moment applied to each modal equation. Ref. [12] and [13] describes how to get the piezoelectric generalized forces in a plate model. We can approximate our beam model as a plate by considering that the deflection at a point x,y is given by:

$$\eta(x,y) = w(x) + y\theta(x), \tag{11}$$

where (x,y) is a position in the plate plane - x is the position along the beam axis, y is the distance to the mean axis. Then, by adaptation of the formulation from Ref. [13] (Eq. 19), the generalized forces in bending and torsion equations due to piezoelectric effect are be obtained as:

$$F_i = \frac{K_{2a}l}{2}\left(\frac{\partial W_i(x_2)}{\partial x} - \frac{\partial W_i(x_1)}{\partial x}\right)v_p \tag{12}$$

$$M_i = \frac{K_{2a} l^2}{8}\left(\frac{\partial \Theta_i(x_2)}{\partial x} - \frac{\partial \Theta_i(x_1)}{\partial x}\right) v_p \tag{13}$$

where $K_{2a} = \frac{\zeta(\zeta+1)}{\frac{1}{1-\nu}+\frac{\beta}{1-\nu_p}(6\zeta+12\zeta^2+8\zeta^3)} \frac{E d_{31} \beta h^2}{(1-\nu)(1-\nu_p) t_p}$, $\beta = E_p/E$, $\zeta = t_p/h$, E is the plate Young modulus, E_p is the piezoelectric Young modulus, d_{13} is the piezoelectric constant, t_p is the patch thickness, h is the plate thickness, l is the beam width, ν is the plate material Poisson's ratio, ν_p is the piezoelectric material Poisson's ratio, x_1 and x_2 are the piezoelectric patches starting and ending positions along the plate, v_p is the applied voltage. In both cases, it is considered a single patch that occupies half of the beam width. Moment equation changes sign depending on the piezoelectric patch position (upper ou lower).

III. SLOSHING DYNAMICS

In this section, we show how we can find a dynamic relationship between translations of the fluid tank and pressures at the tank walls. From these pressures, we can find the resulting force and moment due to sloshing.

Consider the following hypothesis: small perturbations, inviscid and incompressible fluid. From the principle of mass conservation, we have the following equation:

$$\nabla^2 \phi(x, y, z, t) = 0, \tag{14}$$

where ϕ is the velocity potential, so that:

$$\frac{\partial \phi}{\partial x} = v_x, \quad \frac{\partial \phi}{\partial y} = v_y, \quad \frac{\partial \phi}{\partial z} = v_z,$$

where v_x, v_y and v_z are the fluid velocity components at point (x, y, z), in directions x,y and z, respectively.

It is important to notice that we are using a rectangular tank approximation. This approach leads to relatively easy to solve partial differential equations (which is not the case of sloshing in horizontal cylindrical containers). In order to find a good agreement between the sloshing in rectangular and cylindrical tanks, one must consider the same free-surface area as well as the same total volume of fluid.

A. Rectangular tank under lateral oscillations

The tank is moving in the z direction at speed $\dot{\Xi}(t)$. Since the tank walls are considered rigid and impermeable, the following boundary conditions apply:

- At each lateral wall:
$$\frac{\partial \phi}{\partial z} = \dot{\Xi}(t), \quad at \quad z = -a/2 \quad and \quad z = a/2. \tag{15}$$
- At the tank bottom:
$$\frac{\partial \phi}{\partial y} = 0, \quad at \quad y = 0. \tag{16}$$

From Euler equation (moment conservation):

$$\frac{\partial \phi}{\partial t} + g(y-h) + \frac{P}{\rho} + \frac{1}{2}(v_x^2 + x_y^2 + v_z^2) = 0 \tag{17}$$

where P is the pressure, g is the gravity acceleration, h is the fluid height.

Considering the small perturbation hypothesis, we can ignore the quadratic terms:

$$\frac{\partial \phi}{\partial t} + g(y-h) + \frac{P}{\rho} = 0. \tag{18}$$

At the free surface, we have that $P = 0$ and:

$$y = h + \eta, \tag{19}$$

where η is the free-surface displacement relative to equilibrium (note that it is a function of x,y and t). Then, at free-surface, after derivating in respect to time:

$$\frac{\partial^2 \phi}{\partial t^2} + g\dot{\eta} = 0, \quad \text{at} \quad z = h + \eta, \tag{20}$$

with $\dot{\eta} = v_y = \frac{\partial \phi}{\partial y}$ (at $y = h$), then we have the following boundary condition at $y = h$:

$$\frac{\partial^2 \phi}{\partial t^2} + g\frac{\partial \phi}{\partial y} = 0. \tag{21}$$

By using the following variable substitution: $\tilde{\phi} = \phi - z\dot{\Xi}(t)$, we still have a Laplace Equation, but lateral and bottom boundary conditions will be homogeneous. This allows us to solve the problem by variables separation. Following expression satisfies both the Laplace equation and the new boundary conditions:

$$\tilde{\phi}(y, z, t) = \sum_{n=0}^{\infty} \sin(\lambda_n z) \cosh(\lambda_n y) T_n(t). \tag{22}$$

The free-surface condition can allow us to find $T_n(t)$:

$$\frac{\partial^2 \tilde{\phi}}{\partial t^2} + g\frac{\partial \tilde{\phi}}{\partial y} = -z\dddot{\Xi}, \quad at \quad z = h, \tag{23}$$

From Eqs. 22 and 23, after manipulations:

$$\ddot{T}_n(t) + g\lambda_n \tanh(\lambda_n h) T_n(t) = -\frac{4a}{\pi^2} \frac{(-1)^n}{\cosh(\lambda_n h)(2n+1)^2} \dddot{\Xi}. \tag{24}$$

Applying Laplace transform and substituing ω_n^2 by $g\lambda_n \tanh(\lambda_n h)$:

$$\mathcal{L}\{T_n(t)\}(s) = -\frac{4a}{\pi^2 \cosh(\lambda_n h)} \frac{(-1)^n}{(2n+1)^2} \frac{s}{(s^2 + \omega_n^2)} \mathcal{L}\{\ddot{\Xi}\}(s). \tag{25}$$

It is possible to calculate the force due to sloshing as:

$$F_{lat} = b \int_{y=0}^{h} P(y, z = a/2, t) - P(y, z = -a/2, t) dy \tag{26}$$

where $P(y, z, t) = -\rho \frac{\partial \phi}{\partial t}(y, z, t) + g(y-h)$. Then:

$$\mathcal{L}\{F_{lat}\}(s) = -s\mathcal{L}\{\dot{\Xi}\} \left(abh\rho - \sum_{n=0}^{\infty} \frac{8a^3 b \rho \omega_n^2}{g\pi^4 (2n+1)^4} \frac{s^2}{s^2 + \omega_n^2} \right) \tag{27}$$

The moment expression is given by:

$$\begin{aligned} M_{lat} =& b\int_{y=0}^{h} -(h/2-y)\left(P(y,z=a/2,t)\right)dy \\ &- b\int_{y=0}^{h} -(h/2-y)\left(P(y,z=-a/2,t)\right)dy \\ &+ b\int_{z=-a/2}^{a/2} zP(y=0,z,t)dz \end{aligned} \tag{28}$$

After calculating the moment expression and applying Laplace transform we get:

$$\begin{aligned} &\frac{\mathcal{L}\{M_{lat}\}}{\mathcal{L}\{\ddot{\Xi}\}} = -\frac{ba^3\rho s}{12} + \\ &+\sum_{n=0}^{\infty}\frac{\omega_n^2}{g}\frac{8a^3b\rho}{\pi^4(2n+1)^4}\left[\frac{h}{2}-\frac{2a\tanh(\lambda_n h/2)}{(2n+1)\pi}+\frac{g}{\omega_n^2}\right]\frac{s^2}{s^3+\omega_n^2}. \end{aligned} \tag{29}$$

B. Rectangular tank under pitch oscillations

Under forced pitch oscillations given by the pitch-rate $\dot{\theta}$ (around x axis), the following force and moment expressions are obtained:

$$\begin{aligned} &\frac{\mathcal{L}\{F_{pit}\}}{\mathcal{L}\{\dot{\theta}\}} = -s\left(\frac{\rho a^3 b}{12} - \right. \\ &\left.\sum_{n=0}^{\infty}\frac{\omega_n^2}{g}\frac{8a^3b\rho}{\pi^4(2n+1)^4}\left(\frac{h}{2}-\frac{2a\tanh(\lambda_n h/2)}{(2n+1)\pi}+\frac{g}{\omega_n^2}\right)\frac{s^2}{s^2+\omega_n^2}\right) \end{aligned} \tag{30}$$

$$\begin{aligned} &\frac{\mathcal{L}\{M_{pit}\}}{\mathcal{L}\{\dot{\theta}\}} = \frac{ba^3\rho g}{12} \\ &+ s\sum_{n=0}^{\infty}\frac{\omega_n^2}{g}\frac{8a^3b\rho}{\pi^4(2n+1)^4}\left[\frac{h}{2}-\frac{2a\tanh(\lambda_n h/2)}{(2n+1)\pi}+\frac{g}{\omega_n^2}\right]^2\frac{s^2}{s^2+\omega_n^2} \\ &+ s\sum_{n=0}^{\infty}\frac{8a^3b\rho}{\pi^4(2n+1)}\left[\frac{h}{2}-\frac{a\tanh(\lambda_n h/2)}{(2n+1)\pi}+\frac{g}{\omega_n^2}\right] \\ &+ s\sum_{n=0}^{\infty}\frac{8h^3b\rho}{\pi^4(2n+1)^4}\left[\frac{a}{2}-\frac{3h\tanh(\lambda_n h/2)}{(2n+1)\pi}\right] \end{aligned} \tag{31}$$

C. State-space representations

The Laplace transforms previously obtained lead to:

$$\begin{bmatrix} \mathcal{L}\{F\} \\ \mathcal{L}\{M\} \end{bmatrix} = \begin{bmatrix} \frac{\mathcal{L}\{F_{lat}\}}{\mathcal{L}\{\Xi\}} & \frac{\mathcal{L}\{F_{pit}\}}{\mathcal{L}\{\dot{\theta}\}} \\ \frac{\mathcal{L}\{M_{lat}\}}{\mathcal{L}\{\ddot{\Xi}\}} & \frac{\mathcal{L}\{M_{pit}\}}{\mathcal{L}\{\dot{\theta}\}} \end{bmatrix} \begin{bmatrix} \mathcal{L}\{\dot{\Xi}\} \\ \mathcal{L}\{\dot{\theta}\} \end{bmatrix} \tag{32}$$

This can be converted in a state-space representation. The following state-space representation uses the tank lateral and angular accelerations as inputs. Forces and moments due to sloshing are represented as outputs:

$$\dot{X}_{sl} = A_{sl}X_{sl} + B_{sl}u_{sl} \tag{33}$$

$$y_{sl} = \begin{bmatrix} F \\ M \end{bmatrix} = C_{sl}X_{sl} + D_{sl}u_{sl} \tag{34}$$

where $u_{sl} = \begin{bmatrix} \ddot{\Xi} & \ddot{\theta} \end{bmatrix}^T$

D. Including damping in structural and sloshing dynamics

Eqs. 3 and 9 (structural dynamics), and (Eq. 24) (sloshing) are sets of second order undamped systems. Obviously, a real structure (and fluid) has a damped dynamics. Since damping is often related to viscous effects, adding a term proportional to modal rate of change ($\dot{\eta}$) is a usual simplified solution to this problem. By using this approach, modal shapes aren't affected by this "proportional" damping (See Ref. [8] for usual structural dynamics damping and [1] (Chapter 4), [11] (Chapter 3) for sloshing damping).

$$\ddot{\eta}_i + c_i\dot{\eta}_i + \omega_i^2\eta_i = F_i \tag{35}$$

A usual value for the proportional term is $c_i = 2\omega_i\xi$. The values of damping ratio ξ can be fitted from experiments. In this work, we used a damping ratio $\eta_n = 0.01$.

IV. COUPLING FLUID-STRUCTURE EQUATIONS

In the previous sections, we've seen how to obtain a state-space representation for the fluid sloshing in a rectangular tank.

$$\dot{X}_{sl} = A_{sl}X_{sl} + B_{sl}u_{sl} \tag{36}$$

$$y_{sl} = \begin{bmatrix} F \\ M \end{bmatrix} = C_{sl}X_{sl} + D_{sl}u_{sl} \tag{37}$$

where $u_{sl} = \begin{bmatrix} \ddot{\Xi} & \ddot{\theta} \end{bmatrix}^T$. F and M are the force and moment applied by the fluid in the tank due to sloshing.

We can represent the structural dynamics as:

$$\dot{X} = AX + Bu + B_v v \tag{38}$$

$$y = CX \tag{39}$$

where X are the internal modal states, u is a vector including point-force and moment (which is actually equal to y_{sl}), $y = \begin{bmatrix} \dot{\Xi} & \dot{\theta} \end{bmatrix}^T$ is the output linear and angular velocities at a specific point along the beam. v is the input voltage vector in the piezoelectric actuators.

It is possible to manipulate this latter equation, in order to find the acceleration as output, instead of velocities:

$$\begin{aligned} \dot{y} &= \begin{bmatrix} \ddot{\Xi} \\ \ddot{\theta} \end{bmatrix} = C\dot{x} \\ \begin{bmatrix} \dddot{\Xi} \\ \dddot{\theta} \end{bmatrix} &= CAX + CBu + CB_v v \end{aligned} \tag{40}$$

After manipulations, we find a coupled set of linear ordinary differential equations. We can write it in matrix form:

$$\begin{aligned} \begin{bmatrix} \dot{X}_{sl} \\ \ddot{X} \end{bmatrix} &= \begin{bmatrix} A_1 & A_2 \\ A_3 & A_4 \end{bmatrix}\begin{bmatrix} X_{sl} \\ X \end{bmatrix} \\ &+ \begin{bmatrix} B_{sl}(I-CB_{sl}D_{sl})^{-1}CB_v \\ B_v + B(I-D_{sl}CB)^{-1}D_{sl}CB_v \end{bmatrix} v \end{aligned} \tag{41}$$

where: $A_1 = A_{sl} + B_{sl}(I-CB_{sl}D_{sl})^{-1}CBC_{sl}$, $A_2 = B_{sl}(I-CB_{sl}D_{sl})^{-1}CA$, $A_3 = A + B(I-D_{sl}CB)^{-1}C_{sl}$, $A_4 = B(I-D_{sl}CB)^{-1}D_{sl}CA$.

Finally, from the structural modal displacements X and modal shapes, it is possible to find the displacement/velocities/acceleration at any point of the structure.

Above equation can be used to obtain the structural modal frequencies and the frequency response function, which are compared with experimental results in next section.

V. RESULTS

This section shows the comparison between theoretical, numerical and experimental results. Experimental results were obtained by exciting the structure with piezoelectric actuators and measuring the accelerations along the plate with 8 accelerometers. Two kind of sources were used: random and frequency sweep signals. Results were analyzed with SDT Toolbox (Ref. [3]), in order to obtain the modal frequencies, damping and state-space representation. Numerical results were obtained from a formulation developed at ONERA in collaboration with CNAM (Ref. [18]). In all results, tank is 70% filled of water (in liquid height/diameter ratio).

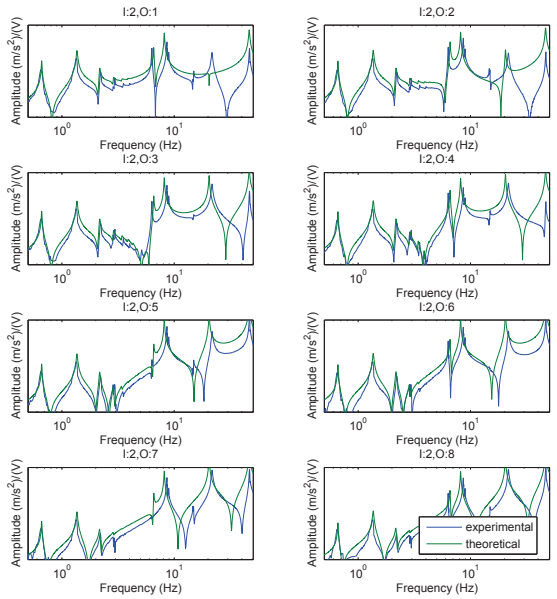

Fig. 2. Theoretical (plate + sloshing) vs experimental (sweep at 50 V) FRF results for each accelerometer (using lower piezoelectric patch). Liquid water.

Fig. 2 shows the frequency response obtained using theoretical model (plate coupled with sloshing) and measured experimentally (frequency sweep of 50 V amplitude). Results are presented for each accelerometer, using the lower piezoelectric patch as input. Table I gives the resonant frequencies obtained from theory, numerical method and experiments.

A few remarks from the results and relationship with original structural and sloshing dynamics:

- 1st mode is closely related to the first bending mode (the frequency value changes considerably from the frozen water to liquid water case, about 0.65 Hz using liquid water, about 0.83 Hz for ice).
- 2nd up to 7th modes are strongly related to sloshing modes. Coupling with first bending modes is visually obvious;
- Our theoretical model wasn't able to predict the 4th (sloshing) mode. When trying to visualize this mode, it is clear it's related with tank yaw motion. This motion wasn't modelled by our sloshing model (we only considered pitch and lateral accelerations);
- 8th mode is closely related to the first torsion mode (6.3 Hz using liquid water, 6.0 Hz using ice);

TABLE I
NATURAL FREQUENCY AND DAMPING RESULTS FOR COUPLED SYSTEM WITH LIQUID WATER

Mode	Theory (Hz)	Numerical (Hz)	Exp. (Hz)	Exp. damping ratio (%)
1 (bend)	0.66	0.64	0.65	1.2
2 (slosh)	1.36	1.36	1.33	1.2
3 (slosh)	2.17	2.12	2.20	0.9
4 (slosh)	NaN	2.83	2.86	4.0
5 (slosh)	2.87	2.90	2.95	0.7
6 (slosh)	3.41	3.38	3.48	59.4
7 (slosh)	3.87	NaN	4.00	42.0
8 (torsion)	6.57	6.56	6.33	0.3
9 (bending)	8.16	9.22	8.68	0.6
10 (??)	NaN	NaN	14.82	0.3
11 (bending)	20.45	24.52	21.91	1.3
12 (bending)	46.52	54.03	47.15	0.6

- 9th mode is the second bending mode (8.7 Hz using liquid water, 7.9 Hz using ice);
- 10th mode is not predicted by any theoretical model; it appears both with liquid water or ice;
- 11th and 12th mode are the third and fourth bending modes.
- System identification of modes 4, 6 and 7 wasn't well acomplished using SDT (values are presented, since an initial choice of natural frequencies are choosen by the user, but damping is unrealistic and agreement of frequency response near these frequencies is not good). It is important to notice, however, that these modes have a very small effect in the measured FRFs;

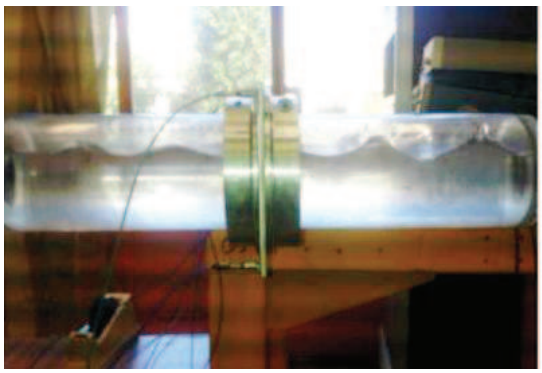

Fig. 3. Large sloshing waves near second bending mode

Nonlinear behavior was clearly observed when exciting the system to large voltages using stepped-sine or frequency sweep near resonant frequencies of the system. Visually, large sloshing waves are observed as those presented in Fig. 3. Fig. 4 shows the different behaviors of the FRF near the second bending mode, for each input signal. It is easy to see that very different responses are obtained, depending on the input amplitude (and method).

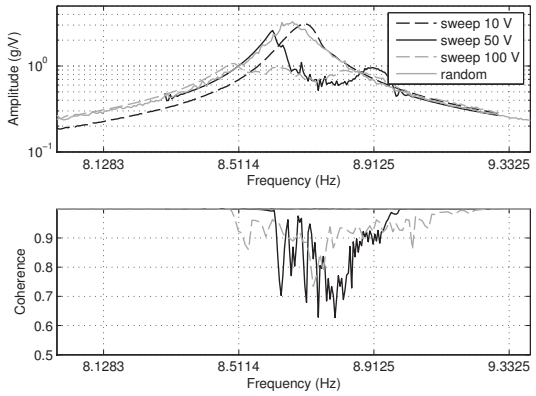

Fig. 4. Frequency response for the system with liquid water in the tank (70% filled) near the second bending mode - voltage amplitude variation - Input:1, Output:2.

- The coherence obtained for frequency sweep inputs using 10 V is almost 1 for the entire frequency range (in this case, sloshing waves are not visually observed for this frequency range);
- When using larger voltages, the coherence between results degradates. This indicates a nonlinear behavior;
- Concerning the coherence obtained for the random signal, it is nearly 1. This happens because during these tests the displacements are small, far from the sloshing nonlinear behavior.

VI. CONCLUSIONS

This article presents the modeling of a coupled fluid-structure system and the results obtained with 3 different methodologies (analytically, numerically and experimentally). The analytical method allows to quickly find a state-space representation of a beam coupled with a fluid-filled rigid tank. Although we used several restrictive hypothesis to find this model, it presented an acceptable agreement with experimental and numerical results. This analytical framework can be used for very simple structures, as well as during early design of structures that can be approximated as a beam coupled with point-masses or point-coupled fluid tanks (like slender high aspect ratio wing with tip tanks). In more complex structures, a fully-numerical schema or experimental tests are needed.

For a high-amplitude excitation, however, nonlinear sloshing waves changes the dynamic behavior of the system and linear hypothesis are no longer valid as seen from experiments. The modeling of the damping, as well as the nature of nonlinear sloshing waves should be better explored in further work.

In addition, our next goal is to use the piezoelectric patches to actively control the system and reduce the system vibrations.

APPENDIX

Experimental data

Fig 5 describes the experimental setup used in this work. Accelerometers are represented as asterisks, marked from 1 to 8. Piezoelectric patches (actuators) are marked as I:1 and I:2. Detailed experimental data are presented in Refs. [16].

Fig. 5. Accelerometers and piezoelectric actuators positions and numbering.

ACKNOWLEDGMENT

This work was partially supported by ANR-project HAMECMOPSYS ANR-11-BS03-0002 and CNPq-Brazil.

REFERENCES

[1] H N Abramson. The Dynamic Behaviour of Liquids in Moving Containers: With Applications to Space Vehicle Technology. Technical report, NASA, 1966.

[2] H. N. Abramson and G. E. Ransleben Jr. Some comparisons of sloshing behaviour in cylindrical tanks with flat and conical bottoms. *ARS Journal - Tecnical Notes*, 31(4):542–568, May 1961.

[3] E Balmes, J Bianchi, and J Leclere. Structural Dynamics Toolbox 6.2 (for use with MATLAB), SDTools, Paris, France, 2009.

[4] H Benaroya and M L Nagurka. *Mechanical Vibration: Analysis, Uncertainties, and Control, Third Edition (Dekker Mechanical Engineering)*. CRC Press, 2009.

[5] J V Burke, D Henrion, A S Lewis, and M L Overton. HIFOO-a MATLAB package for fixed-order controller design and H infinity optimization. In *IFAC Symposium on Robust Control Design*, Toulouse, France, 2006.

[6] J V Burke, D Henrion, A S Lewis, and M L Overton. Stabilization via Nonsmooth , Nonconvex Optimization. *IEEE Transactions on Automatic Control*, 51(11):1760–1769, 2006.

[7] F T Dodge. *The new" dynamic behavior of liquids in moving containers"*. Southwest Research Inst. San Antonio, TX, 2000.

[8] D J Ewins. *Modal testing: theory, practice, and application*. Research Studies Press, 2000.

[9] E W Graham and A M Rodriquez. The characteristics of fuel motion which affect airplane dynamics. Technical report, DTIC Document, 1951.

[10] D H Hodges and G A Pierce. *Introduction to Structural Dynamics and Aeroelasticity*. Cambridge University Press, 2011.

[11] R A Ibrahim. *Liquid Sloshing Dynamics: Theory and Applications*. Cambridge University Press, 2005.

[12] S. Leleu. *Amortissement actif des vibrations d'une structure flexible de type plaque à l'aide de transducteurs piézoélectriques*. PhD thesis, ENS Cachan, 2002.

[13] S. Leleu, H. Abou-Kandil, and Y. Bonnassieux. Piezoelectric actuators and sensors location for active control of flexible structures. *IEEE Transactions on Instrumentation and Measurement*, 50(6):1577–1582, 2001.

[14] L. Meirovitch. *Fundamentals of Vibrations*. McGraw-Hill Science/Engineering/Math, 2001.

[15] S. Mottelet. *Quelques aspectes théoriques et numériques du controle d'un bassin de Carenes*. PhD thesis, Université de Compiègne, 1994.

[16] B. Robu. *Active vibration control of a fluid/plate system*. PhD thesis, Université de Toulouse, Université Toulouse III-Paul Sabatier, 2010.

[17] B. Robu, L. Baudouin, C. Prieur, and D. Arzelier. Simultaneous H infinity Vibration Control of Fluid/Plate System via Reduced-Order Controller. *Control Systems Technology, IEEE Transactions on*, 20(3):700–711, 2012.

[18] J-S Schotté and R Ohayon. Linearized formulation for fluid–structure interaction: Application to the linear dynamic response of a pressurized elastic structure containing a fluid with a free surface. *Journal of Sound and Vibration*, 332(10):2396–2414, 2013.